EURATOM

CEA

ASSOCIATION EURATOM - C.E.A.

DEPARTEMENT DE RECHERCHES SUR LA FUSION CONTROLEE

DRFC-SCP-STGI

EUR-CEA-FC-1264

IDENTIFICATION OF HIGHLY-IONIZED XENON SPECTRA (Xe XXVI through Xe XXXI) EXCITED IN THE PLASMA OF THE TFR TOKAMAK

TFR Group

and

J.F. WYART, C. BAUCHE-ARNOULT, E. LUC-KOENIG

May 1985

Submitted for publication in Physica Scripta

IDENTIFICATION OF HIGHLY-IONIZED XENON SPECTRA (Xe XXVI through Xe XXXI)

EXCITED IN THE PLASMA OF THE TFR TOKAMAK

J.F. Wyart, C. Bauche-Arnoult, E. Luc-Koenig
laboratoire Aimé Cotton, CNRS II, Campus Universitaire
91405 - ORSAY Cedex (France)

and

TFR Group
Association EURATOM - CEA, D.R.F.C., B.P. n°6
F - 92260, FONTENAY AUX ROSES (France)

Abstract

The spectrum of xenon injected into the TFR tokamak plasma has been recorded in the range 10-90 Å by means of a 2m grazing incidence spectrograph. Forty-four lines and unresolved transition arrays pertaining to multicharged xenon ions isoelectronic with Cu I, Ni I, Co I, Fe I, Mn I and Cr I have been identified by means of various theoretical methods. The 17 observed lines of the $3p^6 3d^8$ - $3p^5 3d^9$ transition array, have allowed the wavelengths of the magnetic dipole transitions occuring within the ground configuration $3d^8$ of Xe XXXIX to be predicted.

P.A.C.S. n° 32.20

1. Introduction

Several spectroscopic studies have been devoted so far to the spectra of highly charged xenon since the early observation of three resonance lines (the transitions $4s^2\ ^1S_0 - 4s4p\ ^1P_1$, $4s\ ^2S_{1/2} - 4p\ ^2P_{1/2,\ 3/2}$ of Xe XXV and Xe XXIV respectively) by Hinnov in the ST tokamak [1]. The n = 3 to n = 2 transitions of the sodium-like to oxygen-like xenon (Xe XLIV - Xe XLVII) were excited in laser irradiated microballoons filled with xenon [2] ; the Ne-, Na-, F-like ion transitions have also been seen at higher resolution from xenon ions accelerated in Super-Hilac [3]. Some spectra of moderately charged ions have been investigated in a thetapinch (Xe VIII) and in a low inductance vacuum spark (Xe X) [4, 5]. As a part of systematic investigations, we recently reported on krypton spectra (Kr XVIII through Kr XXIX) observed in TFR in the range 15 - 300 Å [6]. The present article is devoted to similar identifications of Xe XXVI through Xe XXXI in a less extended wavelength range (12-90 Å), including the main $\Delta n = 1$ transitions of these spectra.

2. Experimental conditions

The experiments were performed in ohmically heated TFR tokamak plasmas. The plasma parameters were, during the quasi-staticnary current plateau phase : plasma current I_p = 180 kA, toroidal magnetic field B_T = 4.0 T, working gas H_2, graphite limiter radius a = 19.5 cm, central electron density $n_e(0) = 6.10^{13}\ cm^{-3}$ and central electron temperature $T_e(0) = (1.4 \pm 0.15)$ keV. The spectrum was recorded photographically in the 10-90 Å spectral range by using a 2m radius grazing incidence (1.5°) spectrograph [7] equipped with a 2400 grooves/mm, gold coated, 1° blazed Bausch and Lomb grating. The line of sight of the spectrograph passed through the plasma center and the number of recorded discharges was 100. Intrinsic impurities (C,N,O,Cr,Fe and Ni) provided internal standards used to derive the xenon line wavelengths by polynomial fitting. Spectra obtained from discharges without xenon injection, were used to help in the xenon identifications. The estimated accuracy of our wavelength measurements is between 0.01 and 0.02 Å, depending on the intensity and profile of the line under study.

A vacuum ultraviolet duochromator was used to monitor 3 resonance lines of quasi-central, medium ionization potential ions already identified by Hinnov (Xe XXV $4s^2\ ^1S_0 - 4s4p\ ^1P_1$ at 164.5 Å, = 852 eV and Xe XXVI $4s\ ^2S_{1/2} - 4p\ ^2P_{1/2,3/2}$ at 234.2 Å and 173.9 Å, = 890 eV). Figure 1 shows the temporal evolution of :

a) the plasma current I_p,

b) the central electron temperature $T_e(0)$ from Thomson scattering and the central line electron density $n_e(0)$,

c) the radiance B of the copper-like line at 234.2 Å.

Figure 2 shows the radial profiles, measured at 300 ms, of the electron temperature T_e and of the electron density n_e.

3. Interpretation of the spectrum

At first sight, two spectral regions are important on the spectrogram :

1) below 21 Å, where the wavy shape of the successive unresolved transition arrays (UTA) $3d^N - 3d^{N-1}4p$ and $3d^N - 3d^{N-1}4f$ make xenon spectra very similar to those of molybdenum in the range 22 - 50 Å [8] and

2) between 40 and 55 Å, where several dozens of lines are resolved.

Several methods were used to label the lines and UTA's : a) empirical interpolation or extrapolation of wavenumbers along well-known isoelectronic sequences of Cu I, Ni I and Co I ; b) comparisons of measured lines with the spectrum of copper-like Xe XXVI predicted by the Dirac-Hartree-Fock method [9]; c) comparison of wavenumbers with ab initio evaluation of the energy levels of Xe XXVII and Xe XXVIII, using the parametric potential method [10] ; d) evaluation of the low energy levels of Xe XXIX by means of the Slater-Condon parametric theory ; e) evaluation of the center of gravity and width of the UTA's from the formalism developed in [11] and radial integrals obtained by

means of the parametric potential method [12].
The classified lines and UTA's are collected in Table I.

3.1 The transitions n = 3 to n = 4

The use of the relativistic parametric potential method has led to an unambiguous interpretation of the spectral features below 21 Å, as n = 3 to n = 4 transitions. For the resonance lines of nickel-like Xe XXVII and for the center of gravity of the UTA's, the ab initio estimates are very close to the measured wavelengths. However, due to the presence of strong resonance lines of the intrinsic impurities (the spectra of O VII, O VIII, Fe XVII and Ni XIX are rich in this region), the comparison between experiment and theory is sometimes hampered for xenon ; in particular, lines of O VII and Ni XIX perturb the shape of several xenon UTA's. Like in molybdenum [13], the low plasma density results in the E2 $3d^N - 3d^{N-1}4s$ transitions being observed. The strongest xenon line in the 12-21 Å spectral range belongs to the transition $3d^{10}\ {}^1S_0 - 3d^9 4s(5/2,\ 1/2)\ J = 2$, observed at 20.961 Å and makes the usual designation of "forbidden" quite unappropriate. At slightly lower wavelengths, only the strongest of the predicted $3d^{10}4s\ {}^2S_{1/2} - 3d^9 4s4p$, $J = 1/2, 3/2$ transitions [14] could be observed at 19.137 Å and all strong lines between 19.0 and 20.1 Å are attributed to $3d^9 - 3d^8 4s$ transitions in Xe XXVIII. The relative intensity of the 3d-4s and 3d-4p transitions in Xe XXVIII is under study by means of a collisional-radiative model and will be reported in a future publication [15].

It was checked that the asymetry of the UTA's for $3d^N - 3d^{N-1}4p$ transitions, as evaluated from [16], is negligible ; the pure gaussian broken curves drawn on figure 3a are in a good qualitative agreement with the average wavelength and width of observed arrays. The asymmetry of the $3d^N - 3d^{N-1}4f$ arrays was taken into account in the evaluation of the center of gravity of the UTA's and this was needed to get a satisfactory agreement between theory and observations. It is stressed that the theoretical shift of the center of gravity which results from the asymmetry of the arrays ranges from 0.055 Å (Xe XXXI) to 0.062 Å (Xe XXVIII), i.e. about 2.5 times the full width of the arrays given in Table I.

3.2 The $n = 3$, $\Delta n = 0$ transitions of Xe XXVIII and Xe XXIX.

The three lines of the $3p^6 3d^9 - 3p^5 3d^{10}$ array have been identified by Edlén up to Ag XXI [17] and in six ions from Ba^{29+} to Dy^{39+} by Reader [18]. The wavenumbers derived by parametric interpolation for Xe^{27+} were found within the error bars of three measured lines. The strongest line of the 40-55 Å region is, as expected, the $^2D_{5/2}$ - $^2P_{3/2}$ transition of Xe XXVIII. The weak $^2D_{3/2}$ - $^2P_{3/2}$ line is close to stronger ones of other ions ans the splittings of the ^2D and ^2P terms which we can derive from our measurements are certainly less accurate than the empirical estimates from isoelectronic regularities [18].

The FeI isoelectronic sequence has been extensively studied in the past years. Almost all the levels of $3p^6 3d^8$ and $3p^5 3d^9$ are known from Y XIV to Ag XXII [19] and the strongest transitions 3p-3d could be traced up to Sn XXV [20]. The energy parameters which describe the levels of $3d^8$ within the framework of the Slater-Condon theory have been already determined by generalized-least-squares techniques from all levels of the iron-like ions [19,21]. The constraints on the isoelectronic evolution of these parameters result in a smooth isoelectronic evolution of the residual discrepancies between experimental and theoretical energies. This allows fairly accurate predictions for the levels of the ground configuration $3d^8$ of Xe XXIX shown in Table II. We made use of the results of [19] to calculate energies and eigenfunctions for the 12 levels of $3p^5 3d$ and to derive the 60 possible 3p-3d E1 transitions. By comparing observed intensities and theoretical line strengths, 17 xenon lines could be identified which represent 67% of the total line strength in the transition array. We used the estimated (or experimental whenever possible) energies of $3d^8$ to predict the wavelengths and transition rates of the 14 magnetic dipole lines occurring within $3d^8$, which may be of interest for diagnostics in plasma with low electron density (Table III).

After the interpretation of the main spectral features between

40 and 55 Å, several lines of medium or weak intensity are not yet labeled in the same spectral range. We can infer from the presence of the $3p^6 3d^7 - 3p^6 3d^6 4f$ array around 12.8 Å, that the transitions $3p^6 3d^7 - 3p^5 3d^8$ of the same ion should also show up. Although the latter array has been partly analyzed from Y XV to Ag XXIII [22], isoelectronic extrapolations to Xe XXX did not allow to classify more lines up to now.

There is an obvious similarity between the xenon spectrum on our figure 3 and the spectral region 38-42 Å from a laser-produced samarium plasma (see fig. 1 of [18]), so that we can support Reader's assumption that the unidentified line labeled (e) in [18] belongs to Sm XXXVIII ; more precisely, it is the transition $3p^6 3d^8\ ^3F_4 - 3p^5 3d^9\ ^3D_3$, observed in Xe XXIX at 48.525 Å.

Similarly to the $n = 3$, $\Delta n = 0$ transitions of the magnesium-like Kr XXV and sodium-like Kr XXVI which were remeasured recently [6], the $n = 4$, $\Delta n = 0$ transitions of the zinc-like Xe XXV and copper-like Xe XXVI are strong in the region 100-300 Å. Their wavelength accuracy in [1] is not sufficient to derive a comprehensive level scheme of Xe XXVI and further observations are planned.

REFERENCES

1. Hinnov, E., Phys. Rev. A 14, 1533 (1976).
2. Conturie, Y., Yaakobi, B., Feldman, U., Doschek, G.A. and Cowan, R.D. J. Opt. Soc. Am. 71, 1309 (1981).
3. Dietrich, D.D., Chandler, G.A., Fortner, R.J., Hailey, C.J. and Stewart, R.E., Phys. Rev. Lett. 54, 1008 (1985).
4. Roberts, J.R., Knystautas, E.J. and Sugar, J., J. Opt. Soc. Am. 69, 1620 (1979).
5. Kaufman, V., Sugar, J. and Tech, J., J. Opt. Soc. Am. 73, 691 (1983).
6. Wyart, J.F. and TFR Group, in press (1985).
7. Breton, C., De Michelis, C., Finkenthal, M., and Mattioli, M., J. Opt. Soc. Am. 69 1652 (1979).
8. Schwob, J.L., Klapisch, M., Schweitzer, N., Finkenthal, M., Breton, C., De Michelis, C. and Mattioli, M., Phys. Lett. 62A, 85 (1977).
9. Cheng, K.T. and Kim, Y.K., At. Data and Nuc. Dat. Tab. 22, 547 (1978).
10. Luc-Koenig, E., Physica (Utrecht) 62, 393 (1972) ; Klapisch, M., Schwob, J.L., Fraenkel, B.S. and Oreg, J., J. Opt. Soc. Am. 67, 148 (1977).
11. Bauche-Arnoult, C., Bauche, J. and Klapisch, M. Phys. Rev. A 20, 2424 (1979).
12. Bauche, J., Bauche-Arnoult, C., Luc-Koenig, E., Klapisch, M., J. Phys. B. Atom. Molec. Phys. 15, 2325 (1982).
13. Klapisch, M., Schwob, J.L., Finkenthal, M., Fraenkel, B.S., Egert, S., Bar-Shalom, A., Breton, C., De Michelis, C., and Mattioli, M., Phys. Rev. Lett. 41, 403 (1978).
14. Wyart, J.F., van Kleef, Th.A.M., Ryabtsev, A.N. and Joshi, Y.N. Physica Scripta 29, 319 (1984).
15. Klapisch, M. et al., to be published (1985).
16. Bauche-Arnoult, C., Bauche, J. and Klapisch, M., Phys. Rev. A 30, 3026 (1984).
17. Edlén, B., Atomic Spectra, in Handbuch der Physik, Vol. XXVII Edit. S. Flügge, Springer Verlag, Berlin (1964).

18. Reader, J., J. Opt. Soc. Am. 73, 63 (1983).
19. Wyart, J.F., Klapisch, M., Schwob, J.L., Schweitzer, N. and Mandelbaum, P., Physica Scripta 27, 275 (1983).
20. Kononov, E. Ya., Podobedova, L.I. and Churilov, S.S., Opt. i Spektr. 57, 26 (1984).
21. Wyart, J.F., Uylings, P.H.M. and Raassen, A.J.J., to be published (1985).
22. Wyart, J.F., Klapisch, M., Schwob, J.L. and Mandelbaum, P., Physica Scripta 28, 381 (1983).
23. Edlén, B., Zeit. Phys. 100, 621 (1936).

TABLE I : Classified lines of Xe XXVI - Xe XXXI (12 - 60 Å)

Spectrum	Experimental Wavelength	Experimental Intensity	Theoretical Wavelength	Classification g
Xe XXXI	12.4 n	(5)	12.396 [0.025]a	$3d^6-3d^5 4f$
Xe XXX	12,81 n	(10)	12.795 [0.024]a	$3d^7-3d^6 4f$
Xe XXIX	13.27	(20)	13.250[0.023]a	$3d^8-3d^7 4f$
Xe XXVIII	13.70 n	(30)	13.715[0.020]d	$3d^9-3d^8 4f$
Xe XXVII	14.247	70	14.223b	$3d^{10}\,{}^1S_0-3d^9 4f\,{}^1P_1$
Xe XXVII	14.618	20	14.624b	$3d^{10}\,{}^1S_0-3d^9 4f\,{}^3D_1$
Xe XXXI	15.5	(5)	15.452[0.44]c	$3d^6-3d^5 4p$
Xe XXX	16.2	(5)	16.173[0.46]c	$3d^7-3d^6 4p$
Xe XXIX	17.0	(10)	16.987[0.46]c	$3d^8-3d^7 4p$
Xe XXVIII	17.8 q	(20)	17.821[0.42]c	$3d^9-3d^8 4p$
Xe XXVII	18.326	40	18.333b	$3d^{10}\,{}^1S_0-3d^9 4p\,{}^3D_1$
Xe XXVII	18.667	70	18.675b	$3d^{10}\,{}^1S_0-3d^9 4p\,{}^1P_1$
Xe XXVII	18.826	30	18.836b	$3d^{10}\,{}^1S_0-3d^9 4p\,{}^3P_1$
Xe XXVI	19.137	5	19.144j	$3d^{10} 4s\,{}^2S_{1/2}-3d^9 4s 4p\,{}^2P_{1/2}$
Xe XXVII	20.502	70	20.507b	$3d^{10}\,{}^1S_0-3d^9 4s(3/2,1/2)2$
Xe XXVII	20.961	100	20.964b	$3d^{10}\,{}^1S_0-3d^9 4s(5/2,1/2)2$
Xe XXVI	34.380	5	34.45d	$4p\,{}^2P_{3/2}-5d\,{}^2D_{5/2}$
Xe XXVI	35.61	1	35.71d	$4f\,{}^2F_{5/2}-6g\,{}^2G_{7/2}$
Xe XXVI	35.660	5w	35.75d	$4f\,{}^2F_{7/2}-6g\,{}^2G_{9/2}$
Xe XXVI }	39.410	10	{ 39.52d	$4d\,{}^2D_{3/2}-5f\,{}^2F_{5/2}$
Xe XXIX }			{ 39.385e	$3p^6 3d^8\ 3_1-3p^5 3d^9\ 3^\circ_3$
Xe XXIX	40.335	10	40.433e	$3p^6 3d^8\ 3_1-3p^5 3d^9\ 2^\circ_3$
Xe XXVIII	40.490	30	40.471f	$3p^6 3d^9\,{}^2D_{3/2}-3p^5 3d^{10}\,{}^2P^\circ_{1/2}$
C V }			{ 40.731	$1s^2\,{}^1S_0-1s2p\,{}^1P_1$
Xe XXIX }	40.731	100	{ 40.721e	$3p^6 3d^8\ 4_2-3p^5 3d^9\ 3_3{}^\circ$
Xe XXVI }			{ 40.83d	$4p\,{}^2P_{1/2}-5s\,{}^2S_{1/2}$
Xe XXIX	41.540	5	41.625e	$3p^6 3d^8\ 1_1-3p^5 3d^9\ 2_3{}^\circ$
Xe XXIX	42.310	5	42.299e	$3p^6 3d^8\ 2_3-3p^5 3d^9\ 2_4{}^\circ$
Xe XXVI	43.315	15	43.43d	$4p\,{}^2P_{3/2}-5s\,{}^2S_{1/2}$
Xe XXIX	45.730	15	45.673e	$3p^6 3d^8\ 4_1-3p^5 3d^9\ 3_2$
Xe XXIX	46.615	5w	46.552e	$3p^6 3d^8\ 2_1-3p^5 3d^9\ 1_2$

Xe XXIX	47.970	10	47.879e	$3p^6 3d^8\ 3_1 - 3p^5 3d^9\ 3_2^o$
Xe XXIX	48.115	5	48.031e	$3p^6 3d^8\ 2_1 - 3p^5 3d^9\ 1_1^o$
Xe XXIX	48.525	50	48.512e	$3p^6 3d^8\ 4_1 - 3p^5 3d^9\ 3_1^o$
Xe XXVIII	48.640	100	48.633f	$3p^6 3d^9\ {}^2D_{5/2} - 3p^5 3d^{10}\ {}^2P^o_{3/2}$
Xe XXIX	48.875	5	48.818e	$3p^6 3d^8\ 2_2 - 3p^5 3d^9\ 1_2^o$
Xe XXIX	49.125	20	49.109e	$3p^6 3d^8\ 3_1 - 3p^5 3d^9\ 2_2^o$
Xe XXIX	49.940	15	49.868e	$3p^6 3d^8\ 4_2 - 3p^5 3d^9\ 3_2^o$
Xe XXIX	51.085	50	51.128e	$3p^6 3d^8\ 4_1 - 3p^5 3d^9\ 4_1^o$
Xe XXIX	51.285	20w	51.290e	$3p^6 3d^8\ 2_1 - 3p^5 3d^9\ 2_1^o$
Xe XXVIII	51.355	10	51.353f	$3p^6 3d^9\ {}^2D_{3/2} - 3p^5 3d^{10}\ {}^2P^o_{3/2}$
Xe XXIX	52.220	5	52.203e	$3p^6 3d^8\ 2_2 - 3p^5 3d^9\ 3_1^o$
Ni XVIII Xe XXVI	52.615	10w	52.615h 52.84d	$3d\ {}^2D_{3/2} - 4f\ {}^2F_{5/2}$ $4f\ {}^2F_{5/2} - 5g\ {}^2G_{7/2}$
Ni XVIII Xe XXVI	52.710	30	52.720h 52.93d	$3d\ {}^2D_{5/2} - 4f\ {}^2F_{7/2}$ $4f\ {}^2F_{7/2} - 5g\ {}^2G_{9/2}$
Xe XXIX	53.885	5	53.909e	$3p^6 3d^8\ 3_1 - 3p^5 3d^9\ 4_1^o$
Xe XXVI	54.030	10	54.14d	$4d\ {}^2D_{5/2} - 5p\ {}^2P_{3/2}$
Xe XXVI	55.145	10	55.25d	$4d\ {}^2D_{3/2} - 5p\ {}^2P_{1/2}$

NOTES

a : center of gravity [and width] of the unresolved transition array as calculated in (16) taking into account the asymmetry of the array.

b : wavelength calculated by means of the relativistic parametric potential method.

c : center of gravity [and width] of the unresolved transition array, asymetry being neglected.

d : wavelength calculated by the Dirac-Hartree-Fock method (9).

e : wavelength derived from the Slater-Condon-type parametric study of $3p^6 3d^8$ and $3p^5 3d^9$, without corrections for systematic trends of the discrepancies $\Delta\lambda$ along the isoelectronic sequence.

f : wavelength from empirical interpolation.

g : levels of $3p^6 3d^8$ and $3p^5 3d^9$ are designated by their J-value (indexed from the lowest one of the given J).

h : wavelength measured by Edlen (23).

i : approximate relative observed intensities.

n : blended with a nickel line.

p : blended with an oxygen line.

j : from Wyart et al (14).

w : wide line.

TABLE II : Energy levels of $^{3}d^{8}$, from diagonalization (E_a), corrected for systematic discrepancies (E_b), derived from classified lines (E_{exp}). All values in cm^{-1}.
Eigenfunctions are given in LS coupling
(squarred amplitudes, negative component are underlined)

J N_{th}	E_a	E_b	E_{exp}	Composition
4_1	0	0	0	^3F 0.9372 ^1G 0.0628
2_1	46000	46850		^1D 0.5102 ^3P 0.3253 $\underline{^3F}$ 0.1644
3_1	100910	102160(500)	102110(400)	^3F 1.0000
0_1	127770	127800(1000)		^3P 0.7314 $\underline{^1S}$ 0.2686
2_2	145730	145880(1000)		^3P 0.5288 ^3F 0.4273 $\underline{^1D}$ 0.0439
1_1	171750	172800(1000)	174030?(1000)	^3P 1.0000
4_2	184200	184400(500)	184380(400)	^1G 0.9372 $\underline{^3F}$ 0.0628
2_3	240240	240560(1000)		^1D 0.4458 ^3F 0.4083 $\underline{^3P}$ 0.1459
0_2	374670	374700(1500)		^1S 0.7314 ^3P 0.2686

TABLE III : Predicted magnetic dipole transitions within the ground configuration $3d^8$ of Xe XXIX. Wavelengths are derived from E_{exp} (or E_b) in table II. Transition rates A_{M_1} were calculated from eigenvectors and E_a.

Wavelength in vacuum (Å)	Transition $p^6d^8 - p^5d^9$	A_{M_1} in (s^{-1})
495 ± 5	$1_1 - 0_2$	40350
516 ± 4	$2_1 - 2_3$	600
542.3 ± 2	$4_1 - 4_2$	12400
722.3 ± 7	$3_1 - 2_3$	28400
794 ± 10	$2_1 - 1_1$	14540
979.4 ± 5	$4_1 - 3_1$	25050
1008 ± 5	$2_1 - 2_2$	14000
1056 ± 25	$2_2 - 2_3$	10600
1215 ± 6	$3_1 - 4_2$	730
1476 ± 45	$1_1 - 2_3$	630
1810 ± 30	$2_1 - 3_1$	700
2220 ± 110	$0_1 - 1_1$	1100
2285 ± 75	$3_1 - 2_2$	990
3710 ± 300	$2_2 - 1_1$	200

FIGURE CAPTIONS

Figure 1 : Time evolution of :

a) plasma current I_p

b) central electron temperature $T_e(0)$ (dashed line) central line density $n_e(0)$ (solid line)

c) radiance B of the 234.2 Å copper-like (Xe XXVI) ion line.

Figure 2 : Radial profiles measured at t = 300 ms of the electron temperature T_e (dashed line) and of the electron density n_e (solid line).

Figure 3 : Densitometer tracing of the xenon spectrum:

a) from 12 to 22 Å, the predicted unresolved transition arrays being drawn with arbitrary intensities (dashed line)

b) from 48 to 53 Å

ÉQUIPE T.F.R.

LISTE N° 11 - MISE À JOUR DU 1ER. OCTOBRE 1984

EXPLOITATION PHYSIQUE DE L'EXPÉRIENCE

- COORDINATION	M. CHATELIER J. TACHON
- SECRÉTARIAT SCIENTIFIQUE	P. LECOUSTEY
- CONDUITE DE LA MACHINE	P. BANNELIER M. CHATELIER M. DUBOIS P. GIOVANNONI L. LAURENT J. TACHON
- MESURES MAGNÉTIQUES	J.L. DURANCEAU P. LECOUSTEY
- INTERFÉROMÉTRIE HCN	J.L. BRUNEAU D. VÉRON
- RÉFLECTOMÉTRIE	M. CALDERON R. CANO F. SIMONET
- DIFFUSION THOMSON	J. LASALLE P. PLATZ
- SPECTRES DE NEUTRES	T. HUTTER C. REVERDIN
- MESURES NUCLÉAIRES, X-DURS	A. GÉRAUD G. MARTIN
- RAYONS X-MOUS	L. JACQUET A.L. PECQUET
- SPECTROMÉTRIE (VISIBLE, UV, X-MOUS)	C. BRETON C. DE MICHELIS W. HECQ M. MATTIOLI P. PLATZ J. RAMETTE B. SAOUTIC
- BOLOMÉTRIE	M.H. ACHARD
- SPECTROMÉTRIE DE MASSE, CONDITIONNEMENT DES PAROIS, PLASMA PÉRIPHÉRIQUE	M.H. ACHARD A. GROSMAN F. LINET
- RAYONNEMENT CYCLOTRONIQUE ÉLECTRONIQUE	
A) SPECTROMÉTRIE INFRAROUGE	L. LAURENT R. SOUBARAS
B) ÉTUDES MICROONDES	R. CANO M. CALDERON B. ZANFAGNA

./...

- MESURE DE LA TURBULENCE PAR DIFFUSION THOMSON....... H. BARKLEY, B. DE GENTILE, F. GERVAIS, J. OLIVAIN, A. QUEMENEUR, L. PIGNOL
- SOURCE MODULÉE.................................... J. DRUAUX, M. FOIS, P. GIOVANNONI, T. HUTTER
- INJECTION DE GLACONS.............................. H. DRAWIN, O. LAZARE

CHAUFFAGES ADDITIONNELS

- INJECTION DE NEUTRES.............................. J.F. BONNAL, J. DRUAUX, M. FOIS, P. GIOVANNONI, R. OBERSON, J.P. ROUBIN
- CHAUFFAGE CYCLOTRONIQUE IONIQUE................... J. ADAM, P. BANNELIER, R. BRUGNETTI, A. FISSOLO, D. GAMBIER, H. KUUS
- CHAUFFAGE CYCLOTRONIQUE ÉLECTRONIQUE.............. R. CANO, J.P. CRENN, M. DUBOIS, L. REBUFFI, B. TOURNESAC, B. ZANFAGNA

INFORMATIQUE

- MATÉRIEL.. M. CHARET
- LOGICIEL.. J. BRETON, A. COHEN, C. REVERDIN, J. TOUCHE
- THÉORIE... J. ANDRÉOLETTI, H. CAPES, J. COTSAFTIS, M. DUBOIS, J. JOHNER, E. MASCHKE, M. PAIN, A. SAMAIN

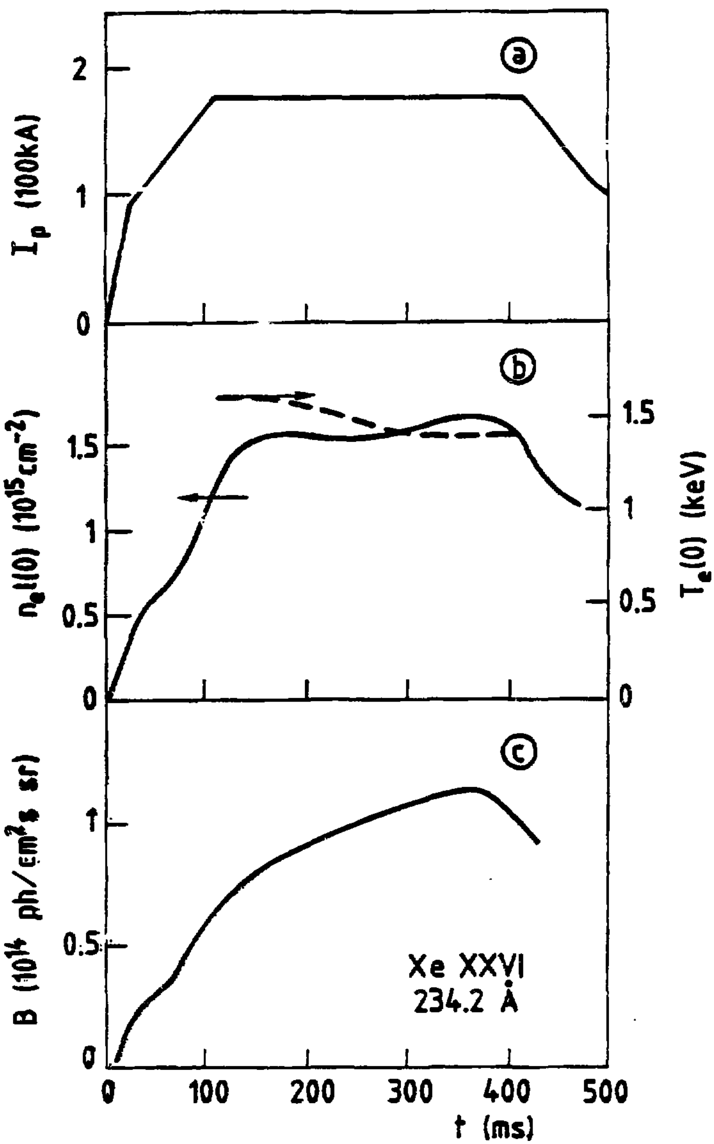

a
b
c
I_p (100kA)
$n_e l(0)$ ($10^{15} cm^{-2}$)
$T_e(0)$ (keV)
B (10^{14} ph/cm^{2}s sr)
Xe XXVI
234.2 Å
t (ms)

Fig. 1

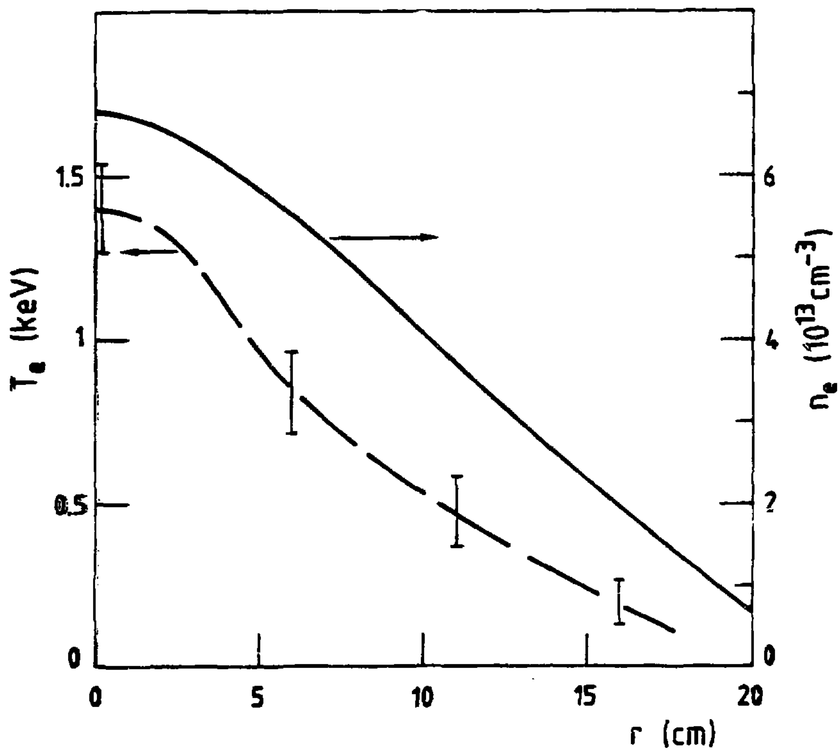

Fig. 2

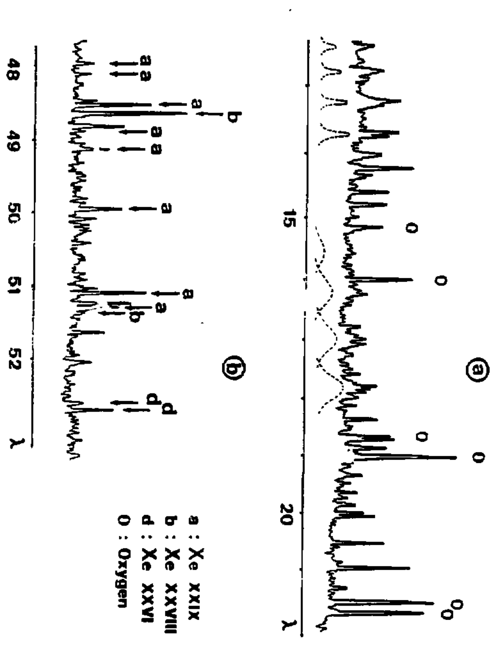

figure 3